

Real-time condition monitoring and fault diagnosis in switched reluctance motors with Kohonen neural network*

Ali UYSAL, Raif BAYIR^{†‡}

(Department of Mechatronics Engineering, Faculty of Technology, Karabük University, Karabük 78050, Turkey)

[†]E-mail: rbayir@karabuk.edu.tr

Received Apr. 9, 2013; Revision accepted Oct. 8, 2013; Crosschecked Nov. 18, 2013

Abstract: The faults in switched reluctance motors (SRMs) were detected and diagnosed in real time with the Kohonen neural network. When a fault happens, both financial losses and undesired situations may occur. For these reasons, it is important to detect the incipient faults of SRMs and to diagnose which faults have occurred. In this study, a test rig was realized to determine the healthy and faulty conditions of SRMs. A data set for the Kohonen neural network was created with implemented measurements. A graphical user interface (GUI) was created in Matlab to test the performance of the Kohonen artificial neural network in real time. The data of the SRM was transferred to this software with a data acquisition card. The condition of the motor was monitored by marking the data measured in real time on the weight position graph of the Kohonen neural network. This test rig is capable of real-time monitoring of the condition of SRMs, which are used with intermittent or continuous operation, and is capable of detecting and diagnosing the faults that may occur in the motor. The Kohonen neural networks used for detection and diagnosis of faults of the SRM in real time with Matlab GUI was embedded in an STM32 processor. A prototype with the STM32 processor was developed to detect and diagnose the faults of SRMs independent of computers.

Key words: Switched reluctance motor, Kohonen neural network, Real-time condition monitoring, Fault detection and diagnosis
doi:10.1631/jzus.C1300085 **Document code:** A **CLC number:** TM32; TP183

1 Introduction

Electric motors convert electrical energy into mechanical energy. Although electric motors are well constructed and reliable, faults may occur while they are operating. Electrical or mechanical faults, or the combination of both, may occur in electric motors. Therefore, in practical applications, safety, reliability, efficiency, and performance of electric motors are the most interesting and specifically important (Vas, 1993; Finley and Burke, 1994; Bayir and Bay, 2007).

Electric machine manufacturers and users take precautions to prevent faults. However, diagnosing the faults that occur inside the motor may take a long

time. Electric motors are getting gradually complicated and these motors are used in applications that have vital importance for people. Breakdown of these motors causes both huge financial losses and the renewal of the machine before its expiration, when the fault is diagnosed but the required precautions are not taken (Isemann, 1997; Nandi and Toliat, 1999; Gao and Ovaska, 2001). Many methods are used in fault detection and diagnosis in electric motors (Liu *et al.*, 2000). One of these is artificial neural networks, which has been used successfully in the field of fault detection and diagnosis (Li *et al.*, 2000; Gao and Ovaska, 2002; Samanta and Al-Balushi, 2003; Bayir and Bay, 2004; Yang *et al.*, 2004).

The Kohonen neural network has been used successfully in numerous engineering fields, including process and system analysis, fault detection, voice recognition, robotics, and pattern recognition (Kohonen *et al.*, 1996). The faults encountered in high

[†] Corresponding author

* Project (No. KBÜ-BAP-C-11-D-003) supported by the Karabük University BAP Unit, Turkey

© Zhejiang University and Springer-Verlag Berlin Heidelberg 2013

voltage energy transferring systems are determined and classified by the artificial neural networks. The voltage and current of high voltage lines are used as input data. The Kohonen network is 100% successful in diagnosing faults encountered in high voltage lines (Chowdhury and Wang, 1996). The Kohonen network is used for fault diagnosis and harmonic analysis of electric motors (Vas, 1999).

A fault detection, diagnosis, and estimation system which is embedded in the field-programmable gate array (FPGA) based platform, is realized using the Kohonen neural network to avoid the maintenance cost of the electrical valve (Gonçalves *et al.*, 2011).

By using Kohonen network spectral data, fault diagnosis of an induction motor was carried out, in which short circuit, unstable and broken rotor bar faults were diagnosed with 100% success (Murray and Penman, 1997). Synchronous generator stator and rotor currents were used to detect the faults using the Kohonen neural network (Jiang and Penman, 1993). Fault diagnosis was realized using the Kohonen neural network and an asynchronous motor vibration signal was processed by fast Fourier transform (FFT) analysis (Penman and Yin, 1994). Asynchronous motor bearing faults using the power source, leakage flux measurement, vibration spectral values, and asymmetry of vibration signals were diagnosed with the Kohonen neural network (Hoffman and van der Merwe, 2002; Kowalski and Orlowska-Kowalska, 2003).

The condition of the starter motor (serial-wound direct current motor) was monitored and fault diagnosis was realized with the Kohonen neural network. The current drawn by the starting motor and voltage across the motor were applied to the Kohonen neural network. With this developed fault diagnosis system, six faults that are seen in starter motors were diagnosed successfully. For fault diagnosis, the GUI software was developed in Visual Basic 6.0 (Bay and Bayir, 2005).

Neural network based control and fault diagnosis were realized for a 6/4 switched reluctance motor. The controller that provides the artificial neural network based optimum speed control was designed. In this controller, the fuzzy logic and traditional proportional-integral (PI) control, and their performance are compared. Back propagation (BP) and self organizing map (SOM) neural networks are used

in detecting the faults of the SRM. It was stated that the control and fault diagnosis program, which was advised for the switched reluctance motor as a result of simulation, showed high performance (Selvaganesan *et al.*, 2006).

A comprehensive method for eccentricity fault diagnosis in the switched reluctance machines during off-line and standstill modes is presented. This sensorless method is able to detect occurrence, location, direction, and severity of the eccentricity fault in the SRM (Torkaman and Afjei, 2013). Chen and Lu (2013) described four main fault types of the asymmetric bridge power converter in the switched reluctance motor drive in power transistors. Two on-line fault diagnosis methods were proposed for power transistors in the power converter. The principle of the proposed diagnosis methods is to detect the real-time current state from some particular positions, and then obtain the diagnosis result and the fault location by logical judgment.

Torkaman *et al.* (2012) have presented a new method for noninvasive diagnosis of static, dynamic, and mixed eccentricity faults in switched reluctance motors. This method makes it possible to precisely determine the features of eccentricity faults. The proposed signature in this algorithm is based on the analysis of the produced current with a particular variation pattern. A novel view of the air-gap magnetic field analysis of a switched reluctance motor under mixed eccentricity was presented to provide a precise fault diagnosis based on a 3D finite element method (Torkaman and Afjei, 2011).

The magnetic characteristics of a switched reluctance motor in healthy and faulty conditions are important in both performance prediction and motor verification. A novel view of air-gap magnetic field analysis of SRM under rotor misalignment was presented (Torkaman *et al.*, 2011). Dorrell and Cossar (2008) have presented a condition monitoring strategy for the detection of rotor eccentricity in switched reluctance machines. It uses vibration measurements and harmonic analysis to generate a Fourier series for the vibrations.

A fuzzy-based control and fault detection system was used for a 6/4 switched reluctance motor (Selvaganesan *et al.*, 2007). The system is realized by primarily doing the simulation of the fuzzy-based fault diagnosis and control system. When a stator

fault occurs in two different SRMs, the fault tolerances of motors were compared (Ruba and Szabó, 2009).

In this study, faults in the SRM are detected and diagnosed in real time with the Kohonen neural network. GUI is used for real-time fault detection and diagnosis in Matlab. To monitor the condition of the motor, the data of the SRM are marked on the weight position graph of the Kohonen neural network. At the same time, the real-time fault detection and diagnosis results are shown on a software screen. The technical specifications of the materials used in experimental study are given and the test rig developed to measure the faulty SRM data is introduced. Results of measurements of SRM faults and details on how they are measured are given. The Kohonen neural network is introduced and the SRM faults are classified in Matlab. The condition of the SRM is monitored with GUI software, which was prepared in Matlab for testing the real-time performance of the Kohonen neural network, and the results of fault diagnosis are given. The Kohonen neural network was embedded in an STM32 processor.

2 Materials and method

2.1 Materials

A test rig was prepared for the real-time fault detection and diagnosis of the SRM using the Kohonen neural network. A block diagram of the test rig is shown in Fig. 1 and the picture of the realized system is shown in Fig. 2.

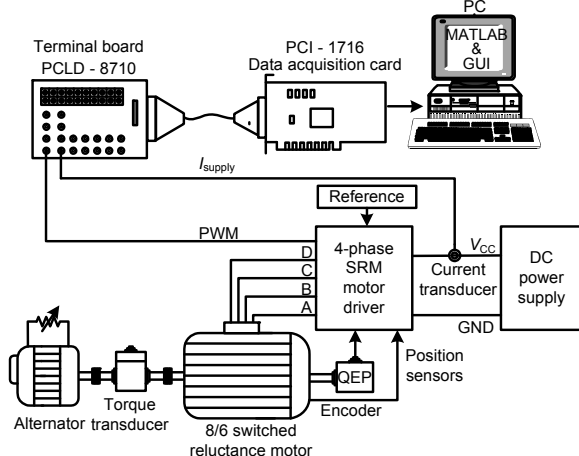


Fig. 1 Block diagram of the test rig

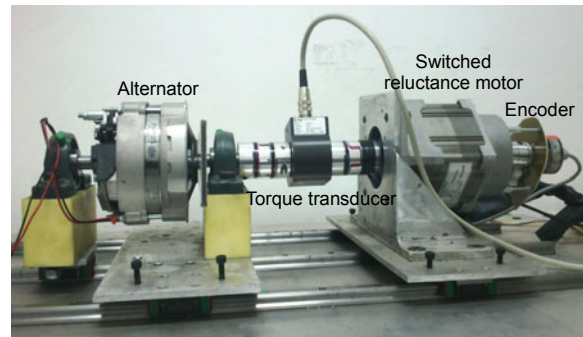


Fig. 2 Picture of the test rig

In this experimental study, a motor with power of 1.34 kW which can be used in low-power industrial applications, was preferred. The technical specifications of the SRM (Rocky Mountain Tech. RA130L) are as follows: It is constructed with 8/6 poles; the maximum torque of the motor is 3.4 N·m and the maximum speed is 15 000 r/min; the supply voltage of the SRM is 96 V; one-phase winding resistance is $R_a=110\text{ m}\Omega$; one-phase inductance when the rotor is at the aligned position is $L_{AL}=2.06\text{ mH}$; one-phase inductance when the rotor is at the unaligned position is $L_{UAL}=0.45\text{ mH}$. The performance graph of the SRM is given in Fig. 3.

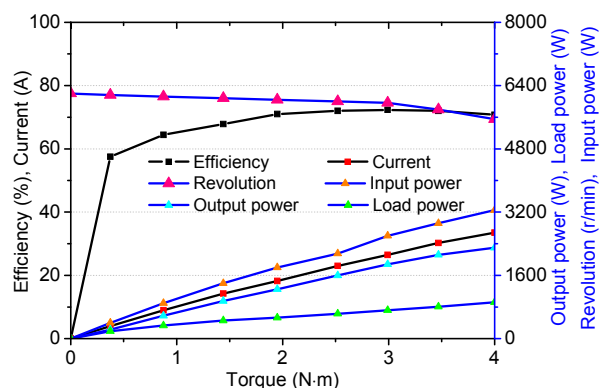


Fig. 3 Dynamic performances and characteristic curves

While the SRM is running at 6000 r/min, it is loaded. In Fig. 3, the motor is loaded with a load which can produce a moment up to 4 N·m. With the torque between 0.5 N·m and 4 N·m, the motor operates with 70% efficiency. The torque produced by the motor increases in proportion to the value of the current it draws. This performance graph is utilized for condition monitoring and fault diagnosis of the SRM.

An asymmetric bridge converter is designed to drive the SRM in the experimental study. As the momentum in the SRM is produced with one-way current, this converter is preferred. Besides, it is the most preferred converter for driving SRMs (Fig. 4). The current for the windings of the asymmetric converter is controlled independently of each other (Duran, 2008).

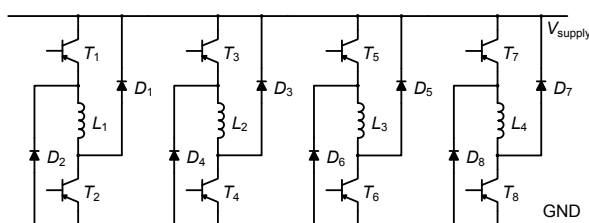


Fig. 4 Asymmetric bridge converter

A torque transducer (ETH Messtechnic DRBK10) is used to measure the torque produced by the SRM. Since the SRM runs at a high speed and can create instantaneous torque changes, the torque sensor with an output response time of 1 ms is preferred. The sensor can measure a speed up to 22 000 r/min. The accuracy of the sensor is 99.5% for 0–10 N·m torque values. The sensor can operate within a 11.5–30 V voltage range. The analog output voltage of the sensor is ± 5 V.

To load the SRM with the desired torque, a synchronous alternator is used as a linear load. The alternator (Mako 55 A) generates 55 A current at 14 V and works with 50% efficiency. With this process, by controlling the excitation winding of the alternator, the SRM is made to work with the desired linear load.

A programmable power supply of TDK-Lambda (100 V, 3.3 kW) is used to provide the operating voltage of the SRM driver, and to run the motor at the maximum power. The output voltage of the power supply can be adjusted within 0–100 V and the output current can be limited to 0–33 A.

To measure the phase current and the total current of the SRM, an LA-55p current transducer with a current conversion ratio of 1:1000 is used. The current sensor has $\pm 99.35\%$ accuracy and $<0.15\%$ linearity value. The response time of the sensor is 1 μ s.

A PicoScope oscilloscope with four channels is used to measure the data of the healthy and faulty conditions of the SRM. The PicoScope is used in

measurement of the duty cycle and the speed during the experimental study. This device has a 12-bit resolution and 20 MS/s sample rate.

The speed of the SRM can be measured by a position sensor with a resolution of 48 pulses/revolution. To measure the motor revolution more precisely, a quadratic encoder with a higher resolution is used. This encoder has a resolution of 1024 pulses/revolution.

To transfer the data into Matlab in real time, an Advantech PCI-1716 data acquisition card is used. This card has a maximum of 250 kS/s sample rate and 16-bit resolution.

In many industrial applications, SRMs are used within a speed range of 500–50 000 r/min and a power range of 100 W–300 kW. SRMs are generally manufactured with 12/8, 8/6, 6/4, 6/2, or 4/2 poles. The inductance of SRMs changes in accordance with the positions of the stator and rotor. When the rotor position is aligned, the inductance reaches its highest value. When the poles are in unaligned positions, the inductance of that phase is at its lowest value.

The basic equivalent circuit for the SRM is obtained by neglecting the common inductance between phases. The voltage applied to one phase is equal to the sum of the voltage drop across the winding resistance and the change in winding flux (Miller *et al.*, 1990).

The voltage with respect to the one-phase equivalent circuit of the SRM (Fig. 5) obtained from induced electromagnetic force (EMF) expressions is

$$v = R_s i + \frac{d\varphi(\theta, i)}{dt}, \quad (1)$$

where R_s is the phase resistance and φ is the phase magnetic flux.

$$\varphi = L(\theta, i)i. \quad (2)$$

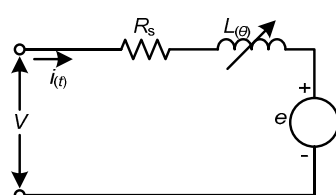


Fig. 5 One-phase equivalent circuit of the SRM

In Eq. (2), L is the inductance which depends on the rotor position and phase current. One-phase voltage is given as

$$v = R_s i + \frac{d\{L(\theta, i)\}}{dt} = R_s i + L(\theta, i) \frac{di}{dt} + i \frac{d\theta}{dt} \frac{dL(\theta, i)}{d\theta}, \quad (3)$$

or

$$v = R_s i + L(\theta, i) \frac{di}{dt} + \frac{dL(\theta, i)}{d\theta} \omega_m i. \quad (4)$$

In Eq. (4), $R_s i$ represents the ohmic voltage drop, $L(\theta, i) \frac{di}{dt}$ represents the inductive voltage drop, and $\frac{dL(\theta, i)}{d\theta} \omega_m i$ represents the induced EMF. Instantaneous input power P_i is calculated as

$$P_i = vi = R_s i^2 + \frac{d}{dt} \left(\frac{1}{2} L(\theta, i) i^2 \right) + \frac{1}{2} i^2 \frac{dL(\theta, i)}{dt}, \quad (5)$$

where $R_s i^2$ is the winding ohmic loss, $\frac{d}{dt} \left(\frac{1}{2} L(\theta, i) i^2 \right)$ is the change rate of field energy, and $\frac{1}{2} i^2 \frac{dL(\theta, i)}{dt}$ is the air-gap power (P_a). The torque of the motor is calculated as

$$T_e = \frac{1}{2} i^2 \frac{dL(\theta, i)}{d\theta}. \quad (6)$$

The total torque of the SRM is equal to the sum of the torque produced by each phase:

$$T_{\text{Total}} = T_{ea} + T_{eb} + T_{ec} + T_{ed}. \quad (7)$$

The motor has four phases and in each phase there are two coils wound on reciprocal stator poles to support the fluxes of each other (Fig. 6). This connection could be either in series or in parallel. When the voltage is applied to the coils, the stator pulls the rotor pole towards itself. When the voltage is supplied to the stator phases consecutively with certain intervals, rotor rotational motion is realized (Duran, 2008).

The inductance of the SRM depending on rotor position and current is calculated by Eq. (8). The expression of inductance is created by adding a

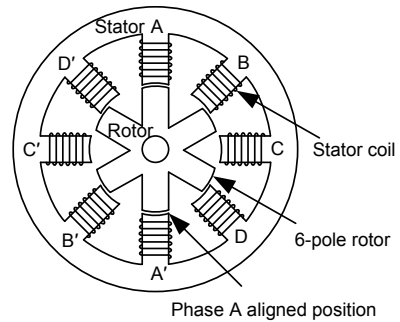


Fig. 6 An 8/6-pole SRM intersection

Gaussian function dependent on the current and rotor position to the minimum inductance (Ustun, 2009).

$$L(\theta, i) = L_u + \frac{L_a - L_u}{1 + i_{pu}} \exp \left[- \left(\frac{\theta_{pu} - n}{\sigma} \right)^2 \right]. \quad (8)$$

In Eq. (8), L is the phase inductance change, L_u is the minimum inductance, $L_a + L_u$ is the maximum inductance, i_{pu} is the current per unit, θ_{pu} is the rotor position per unit, n is the mean of the Gaussian function, and σ is the width of the Gaussian function. The inductance of a phase obtained depending on the rotor position and phase current is given in Fig. 7.

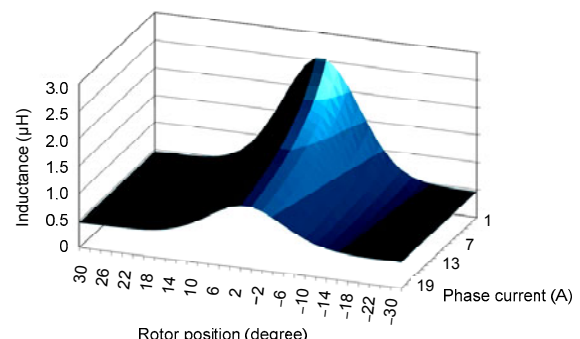


Fig. 7 Phase inductance variation graph for simulation

2.2 Method

2.2.1 Measurement of the SRM faults

In SRMs, mechanical faults, electrical faults, or a combination of these two may occur. An open circuit of one or more phases and rotor locking are the most commonly encountered faults. When SRMs do not run under the maximum load, in the case of one- or two-motor-phase open circuit faults, the motor keeps

running. Hence, before the complete motor breakdown, this situation should be detected and repaired. The output voltages of the sensors used in this study are between 0 and 2.5 V. A passive low-pass filter is used to suppress the switching frequency noise of the sensor outputs. Therefore, the outputs of the sensors are appropriate for the inputs of both the data acquisition card and the STM32 processor.

By running the SRM intermittently, measurements are realized when the motor is in a healthy condition and when one- or two-motor-phase open circuit faults have occurred. These measurements are realized by loading 2 N·m torque when the motor is at 1400 r/min under a healthy operating condition. The revolution, current, and duty cycle of the SRM are given in Fig. 8.

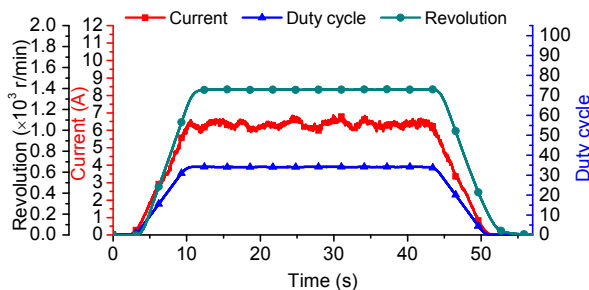


Fig. 8 Healthy condition

The measured revolution, current, and duty cycle are given in Fig. 9 when a one-phase open circuit fault has occurred in the SRM. When the healthy operating condition and a one-phase open operating condition are compared, it is seen that the average of a motor's stable load or motor current in revolution does not change much. In the SRM, when an open circuit fault of one phase (phase A) occurs, to produce the normal torque, the average torque produced by the other three phases (T_{eb} , T_{ec} , T_{ed}) increases (Eq. (9)). Consequently, currents of these phases increase.

$$T_{\text{Total}} = 0 + T_{eb} + T_{ec} + T_{ed}. \quad (9)$$

The torque produced by the SRM depends on the current drawn from the source. In this case, since the total current does not change much, the current drawn from each phase increases when a fault in motor phases occurs under a stable torque. By running the SRM at 1, 1.5, or 2 N·m torque at a reference speed of

1400 r/min under the SRM's healthy and faulty conditions, the current, duty cycle, and revolution parameters are measured using the PicoScope3424.

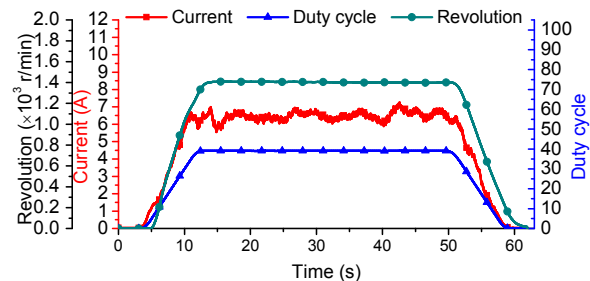


Fig. 9 One-phase open circuit condition

With the SRM's two-phase open circuit, if it is compared with a one-phase open circuit condition, it is seen that the average of the current drawn does not change. When the SRM runs in two phases, the current drawn from the source is divided into two phases to produce the desired torque. Therefore, the value of the pulse width modulation (PWM) duty cycle is seen to have increased more (Fig. 10). In the SRM, when an open circuit fault of two phases (phases A and C) occurs, to produce the normal torque, the average torque produced by the other two phases (T_{eb} , T_{ed}) increases (Eq. (10)). Consequently, the current of these phases increases.

$$T_{\text{Total}} = 0 + T_{ec} + 0 + T_{ed}. \quad (10)$$

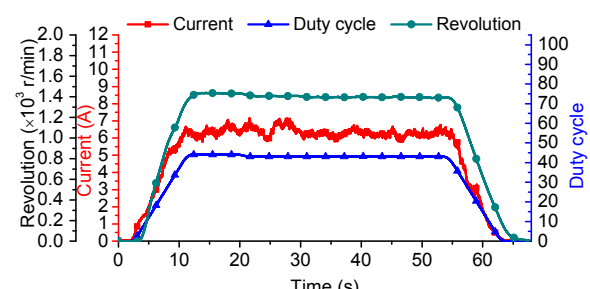


Fig. 10 Two-phase open circuit condition

In the SRM, when an open circuit fault of one phase or two phases occurs, since the average torque produced by the motor does not change, there will not be a large change in the total current drawn from the power source.

The motor current is limited to 10 A when the motor runs in a locked rotor condition. Although the motor driver draws the maximum current from the

source and the PWM duty cycle is at its maximum, the speed of the motor cannot reach the reference value (Fig. 11).

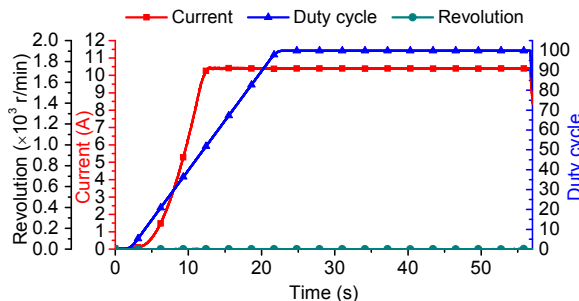


Fig. 11 Locked rotor condition

2.2.2 Classification of SRM faults with the Kohonen neural network

Artificial neural networks are commonly used in fault diagnosis of electric motors. The classification success rate of the Kohonen neural network is very high among artificial neural networks. Besides, compared with other neural networks, the Kohonen neural network requires fewer parameters but works faster. When the previous studies are analyzed, it can be seen that it is usually preferred in the classification of electric devices and driver faults. For this reason, the Kohonen neural network is preferred for real-time fault detection and diagnosis in SRMs.

2.2.3 Kohonen neural network

The Kohonen neural network is an SOM unsupervised-training network. This network structure was developed by Kohonen (2001). The Kohonen neural network has two layers, an input layer and an output layer.

Neural neurons in the output layer are connected with each other and also with the neurons in the input layer. When the network runs, weights are randomly assigned. When the input data is applied, the network starts to carry out its function. It gains a neuron as a result of the training. Inside the border where the neighborhoods of this neuron are decided, neuron weights are changed. As a result, an area is marked which includes the neural network group (Fig. 12). The Kohonen network is divided into two, as one and two dimensional (Haykin, 1999).

The Kohonen neural network algorithm is given below. Since the number of layers of the network is

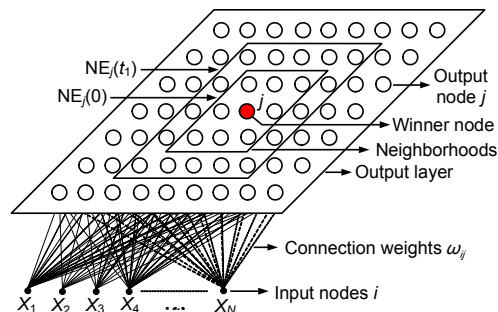


Fig. 12 Kohonen network structure

low and the network is easy to compute, the speed of the network is high. Before the network algorithm is processed, values must be assigned to the constants of neighborhood amount NE_j and gain term η (learning speed).

1. Determine the weights. Small random values are assigned for connections among N input nodes and M output nodes.
2. The input is applied to the network.
3. Distances among all nodes are calculated. Distance between the input and an output node (j), d_i , is calculated by

$$d_i = \sum_{i=0}^{N-1} (x_i(t) - \omega_{ij}(t))^2, \quad (11)$$

where $x_i(t)$ is the i th input node, t is the time, and $\omega_{ij}(t)$ is the weight at time t between the i th input node and j th output node.

4. The output node that has the shortest distance is selected. The selected output node j^* is the node that has the shortest distance, d_i .

5. The weights of node j^* and its neighbors are renewed. $NE_j(t)$ weights of node j^* and its neighboring nodes are renewed:

$$\omega_{ij}(t+1) = \omega_{ij}(t) + \eta(t)(x_i(t) - \omega_{ij}(t)), \quad (12)$$

$$j \in NE_j(t), 0 \leq j \leq N-1,$$

where $\eta(t)$ ($0 < \eta(t) < 1$) is the gain term which decreases with time.

6. Go back to the second step and the process is repeated (Lippmann, 1987).

The Kohonen network is generally used in classification. These networks' ability to both classify the

input vectors and learn the distribution of input vectors is very high (Lippmann, 1987; Fausett, 1994; Haykin, 1999). The Kohonen network is easily defined with the neural network toolbox in Matlab. By presenting sample data to the neural network, the training of the network is realized; by presenting test data to the trained network, the performance of the network is tested. Users can perform the coding related to the network themselves or they can prepare the network via GUI (with the neural network toolbox).

In this study, we aim to realize fault detection and diagnosis of SRMs using a minimum number of input variables. By analyzing the healthy and faulty data sets, the SRM's total current and PWM duty cycle are chosen as the input parameters for the Kohonen neural network. Current is the most used parameter in the detection of motor faults and is directly related to the torque and rotational speed in direct current motors (Chow, 1997). The PWM signal is continuously changed by a controller to provide

desired torque or rotational speed for the motor. A fault occurring in the motor or a change in the load of the motor causes changes in the current drawn by the motor and in the PWM duty cycle. Classification of those changes with the Kohonen neural network, fault detection, and diagnosis of the motor are realized.

The SRM is operated at 1, 1.5, or 2 N·m torque in the condition of healthy, one-phase open circuit, two-phase open circuit, or locked rotor. The Kohonen neural network is defined by 10 000 data in a total of 10 sample data sets in Matlab. Winning neural cells at the outputs of the identified neural network are given in Fig. 13, showing the winning cells of the Kohonen neural network and the number of samples of the winner cells under different fault conditions. Here, when the SRM is in the healthy condition, the winner output neural cells are the 8th, 11th, and 12th cells for 3000 sample data. Table 1 shows winner output cells hit by the faults of the Kohonen neural network according to the motor conditions.

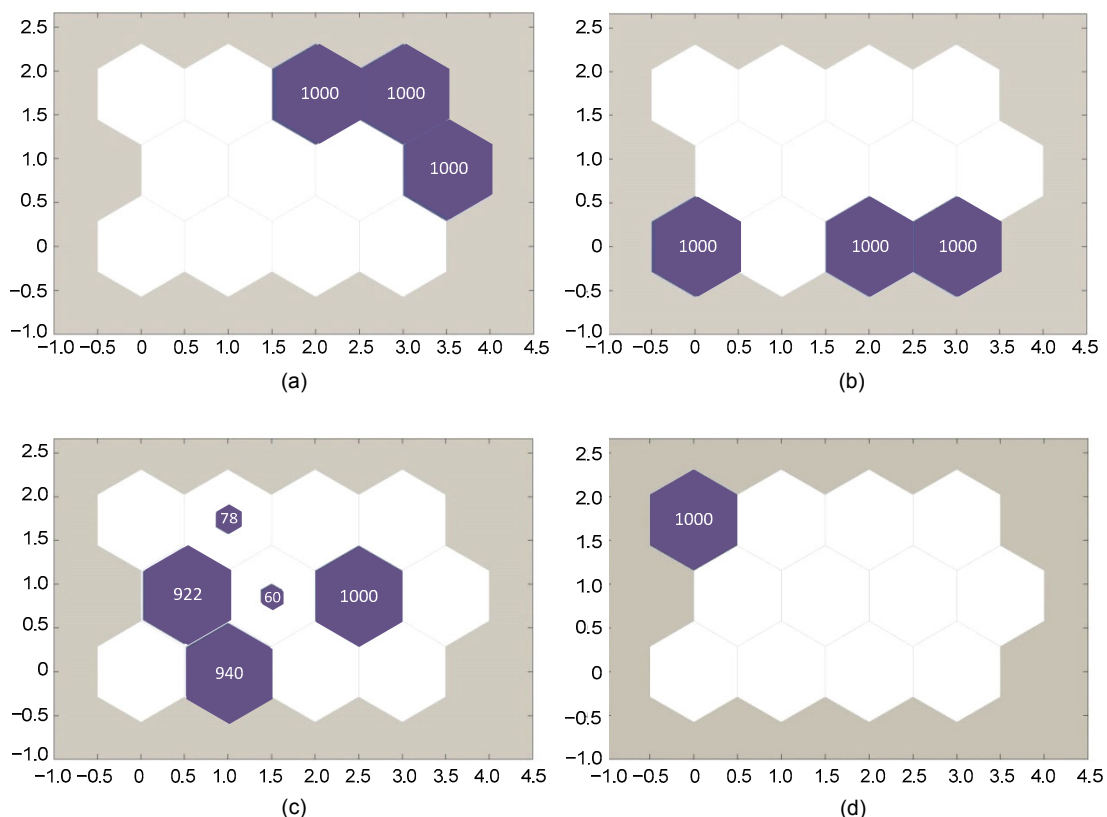


Fig. 13 Active neurons hit under different motor conditions

(a) Healthy condition; (b) One-phase open circuit; (c) Two-phase open circuit; (d) Locked rotor

Table 1 Active output cells of the Kohonen neural network according to the motor condition

No.	Condition	SOM winner neuron(s)
1	Healthy	8, 11, 12
2	One-phase open circuit	1, 3, 4
3	Two-phase open circuit	2, 5, 6, 7, 10
4	Locked rotor	9

This winner cell pointing out the corresponding error is shown in the PWM versus current graph (Fig. 14). Kohonen neural network faults are placed in 200 iterations on the weight position graph. To classify the healthy and faulty situations, the Kohonen neural network output is chosen as 4×3 neurons. SOM weight positions obtained at the end of the training are given in Fig. 14.

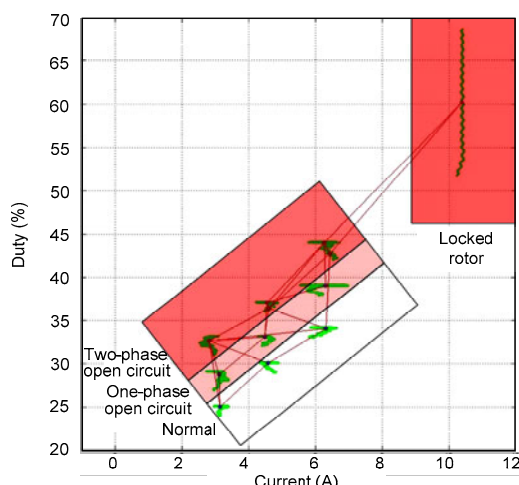


Fig. 14 SOM weight position

Software in Matlab GUI is realized for real-time condition monitoring and fault detection in SRMs (Fig. 15). This software, by pressing the start button, takes data via the data acquisition card and determines the SRM's operating condition. Real-time operation is stopped by pushing the stop button. The current taken via the data acquisition card and the PWM duty cycle are displayed at the left side of the screen. The working condition of SRM's motor is displayed at the right side of the interface.

In the software, the current and PWM duty cycle data acquired in real time from the data acquisition card are applied to the Kohonen neural network. The average of 5000 samples acquired per second through the analog input is applied to the neural network. The

Kohonen neural network classifies the obtained data. As a result of the classification, the SRM's condition is detected in real time. The data used in the classification is marked in real time on the SOM weight position graph. The Kohonen neural network produces 46 results per minute in real time. Thus, the SRM's condition is monitored in real time and in case of a fault, the fault type is monitored by the interface program. For instance, SOM weight positions and the current-PWM duty cycle graph in case of a two-phase open circuit fault are shown in Fig. 16. The Kohonen neural network prepared for the Matlab Simulink model is given in Fig. 17. In the model, an STM 32 Discovery 32-bit ARM Cortex Processor prototype is embedded in the card (Fig. 18).

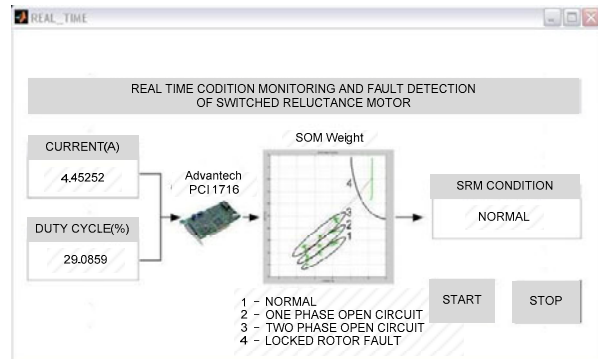


Fig. 15 Matlab GUI real-time fault detection and diagnosis software window

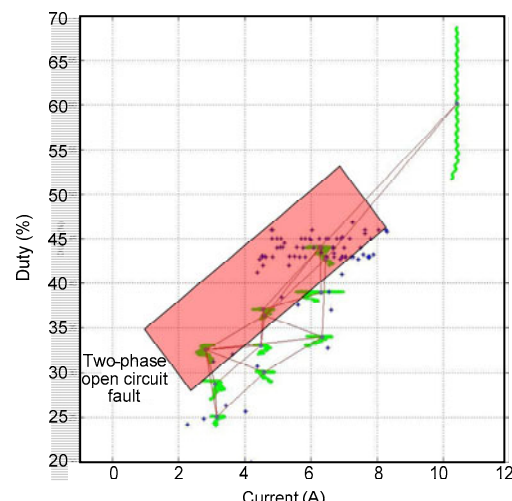


Fig. 16 SOM weight positions and the current-PWM duty cycle graph for a two-phase open circuit fault

* represents the current/PWM duty cycle condition point

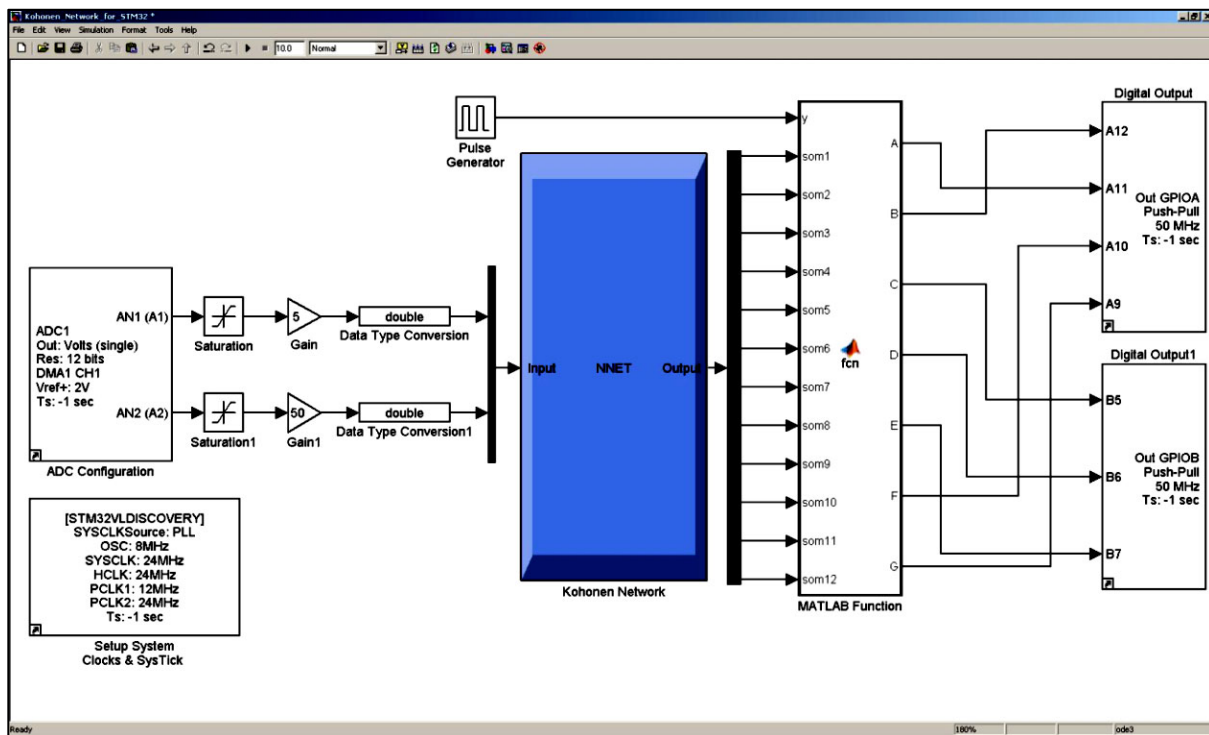


Fig. 17 Matlab model of Kohonen neural network for fault detection and diagnosis prototype

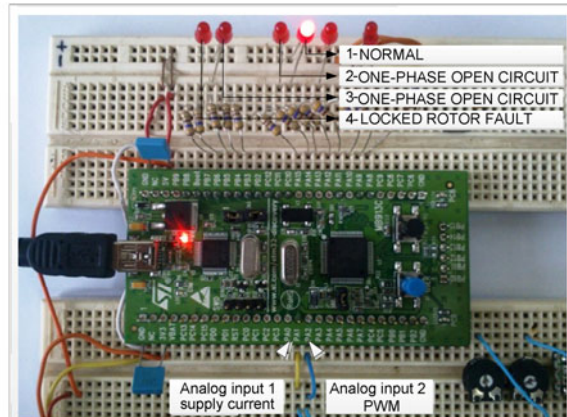


Fig. 18 STM 32 Discovery 32-bit ARM Cortex Processor prototype module

Matlab Real-Time Windows Target Library is used in the process of embedding the model into the STM32 Discovery card. With this prototype, repair, maintenance workshops, and SRM can be used in applications.

3 Results

The performance of the Kohonen neural network used in condition monitoring and fault detection

software was tested using training data, and a 100% success rate was achieved. Real-time performance of condition monitoring and fault diagnosis realized in GUI software is given in Table 2. The software was tested with a total of 335 samples (292 correct and 43 faulty) for a motor's four situations. It is seen that the software was able to detect the situation of the motor with a success ratio of 87%. The reason why the detection ratio under a locked rotor condition is relatively high is that it is away from the other faults in SOM weight positions. The reason why the detection ratio under a one-phase open circuit condition is relatively low is that SOM weight positions are

Table 2 Real-time fault detection and diagnosis software performance

Motor situation	Sample number	Measured sample number		Success percentage
		Correct classification	Wrong classification	
Healthy	77	67	10	87%
One-phase open circuit	92	76	16	82%
Two-phase open circuit	81	70	11	86%
Locked rotor	85	79	6	93%
Total	335	292	43	87%

between the two-phase open circuit and healthy conditions and close to these conditions.

The mode function was used in the application of the embedded system of the Kohonen neural network to increase the success rate (87%). With the mode function, most of the faults produced by the Kohonen neural network per unit time were expressed as the fault of the SRM. In this way, a success rate of 100% was achieved in the embedded system fault detection and diagnosis prototype realized by the STM32 processor.

4 Conclusions

In this study, the motor current and PWM duty cycle data was recorded under SRMs' healthy and faulty operating conditions. Using this data, the Kohonen neural network training was realized. In Matlab GUI, a software GUI was prepared for the detection and diagnosis of faults in the SRM. This software applies the data obtained from the data acquisition card in real time to the Kohonen neural network. Using this software, the SRM's condition is monitored and the fault detection and diagnosis can be realized before the SRM becomes completely broken. The efficiency of the real-time fault detection and diagnosis of the software was 87%. This system can be a prototype using the STM32-Discovery board. It will be a low cost system for condition monitoring and fault diagnosis because of having fewer input variables and requiring only one current sensor. The prototype for detection and diagnosis of faults in SRMs developed in this study can be integrated into a motor driver. In this way, an intelligent motor driver is realized to observe the condition of the motor.

References

- Bay, Ö.F., Bayir, R., 2005. Kohonen network based fault diagnosis and condition monitoring of pre-engaged starter motors. *Int. J. Autom. Technol.*, **6**(4):341-350.
- Bayir, R., Bay, Ö.F., 2004. Serial Wound Starter Motor Faults Diagnosis Using Artificial Neural Network. IEEE Int. Conf. on Mechatronics, p.194-199. [doi:10.1109/ICMECH.2004.1364436]
- Bayir, R., Bay, Ö.F., 2007. Fault diagnosis in starter motors by classification of wavelet analysis results of faulty starter motor's current signals using fuzzy logic. *J. Fac. Eng. Arch. Gazi Univ.*, **22**(2):363-374 (in Turkish).
- Chen, H., Lu, S.L., 2013. Fault diagnosis digital method for power transistors in power converters of switched reluctance motors. *IEEE Trans. Ind. Electron.*, **60**(2):749-763. [doi:10.1109/TIE.2012.2207661]
- Chow, M.Y., 1997. Methodologies of Using Neural Network and Fuzzy Logic Technologies for Motor Incipient Fault Detection. World Scientific, Singapore, p.63-78.
- Chowdhury, B.H., Wang, K.Y., 1996. Fault Classification Using Kohonen Feature Mapping. Int. Conf. on Intelligent Systems Applications to Power Systems, p.194-198. [doi:10.1109/ISAP.1996.501067]
- Dorrell, D.G., Cossar, C., 2008. A vibration-based condition monitoring system for switched reluctance machine rotor eccentricity detection. *IEEE Trans. Magn.*, **44**(9):2204-2214. [doi:10.1109/TMAG.2008.2000498]
- Duran, F., 2008. Intelligent Control of Industrial Washing Machine Uses Switched Reluctance Motor. PhD Thesis, Gazi University Informatics Institute, Ankara, Turkey (in Turkish).
- Fausett, L., 1994. Fundamentals of Neural Networks. Prentice Hall Inc., USA.
- Finley, W.R., Burke, R.R., 1994. Troubleshooting motor problems. *IEEE Trans. Ind. Appl.*, **30**(5):1383-1397. [doi:10.1109/28.315253]
- Gao, X.Z., Ovaska, S.J., 2001. Soft computing methods in motor fault diagnosis. *Appl. Soft Comput.*, **1**(1):73-81. [doi:10.1016/S1568-4946(01)00008-4]
- Gao, X.Z., Ovaska, S.J., 2002. Genetic algorithm training of Elman neural network in motor fault detection. *Neur. Comput. Appl.*, **11**(1):37-44. [doi:10.1007/s005210200014]
- Gonçalves, L.F., Bosa, J.L., Balen, T.R., Lubaszewski, M.S., Schneider, E.L., Henriques, R.V., 2011. Fault detection, diagnosis and prediction in electrical valves using self-organizing maps. *J. Electron. Test.*, **27**(4):551-564. [doi:10.1007/s10836-011-5220-0]
- Haykin, S., 1999. Neural Networks: a Comprehensive Foundation. Prentice Hall Inc., USA.
- Hoffman, A.J., van der Merwe, N.T., 2002. The application of neural networks to vibrational diagnostics for multiple fault conditions. *Comput. Stand. Interface.*, **24**(2):139-149. [doi:10.1016/S0920-5489(02)00014-4]
- Iseemann, R., 1997. Fault-detection and fault-diagnosis methods an introduction. *Control Eng. Pract.*, **5**(5):639-652. [doi:10.1016/S0967-0661(97)00046-4]
- Jiang, H., Penman, J., 1993. Using Kohonen Feature Maps to Monitor the Condition of Synchronous Generators. Workshop on Neural Network Applications and Tools, p.89-94. [doi:10.1109/NNAT.1993.586058]
- Kohonen, T., 2001. Self-Organizing Map (3rd Ed.). Springer Verlag, Germany.
- Kohonen, T., Oja, E., Simula, O., Visa, A., Kangas, J., 1996. Engineering applications of the self-organizing map. *Proc. IEEE*, **84**(10):1358-1384. [doi:10.1109/5.537105]
- Kowalski, C.T., Orlowska-Kowalska, T., 2003. Neural networks application for induction motor faults diagnosis. *Math. Comput. Simul.*, **63**(3-5):435-448. [doi:10.1016/S0378-4754(03)00087-9]

- Li, B., Chow, M.Y., Tipsuwan, Y., Hung, J.C., 2000. Neural-network-based motor rolling bearing fault diagnosis. *IEEE Trans. Ind. Electron.*, **47**(5):1060-1069. [doi:10.1109/41.873214]
- Lippmann, R.P., 1987. An introduction to computing with neural nets. *IEEE ASSP Mag.*, **4**(2):4-22. [doi:10.1109/MASSP.1987.1165576]
- Liu, X.Q., Zhang, H.Y., Liu, J., Yang, J., 2000. Fault detection and diagnosis of permanent-magnet dc motor based on parameter estimation and neural network. *IEEE Trans. Ind. Electron.*, **47**(5):1021-1030. [doi:10.1109/41.873210]
- Miller, T.J.E., Stephenson, J.M., MacMinn, S.R., Handersot, J.R., 1990. Switched Reluctance Drives. IEEE/IAS Annual Meeting.
- Murray, A., Penman, J., 1997. Extracting useful higher order features for condition monitoring using artificial neural networks. *IEEE Trans. Signal Process.*, **45**(11):2821-2828. [doi:10.1109/78.650108]
- Nandi, S., Toliyat, H.A., 1999. Condition Monitoring and Fault Diagnosis of Electrical Machines—a Review. 34th IAS Annual Meeting, p.197-204. [doi:10.1109/IAS.1999.799956]
- Penman, J., Yin, C.M., 1994. Feasibility of using unsupervised learning, artificial neural networks for the condition monitoring of electrical machines. *IEE Proc.-Electr. Power Appl.*, **141**(6):317-322. [doi:10.1049/ip-epa:19941263]
- Ruba, M., Szabó, L., 2009. Fault tolerance study of switched reluctance machines by means of advanced simulation techniques. *Pollack Periodica*, **4**(2):107-116. [doi:10.1556/Pollack.4.2009.2.11]
- Samanta, B., Al-Balushi, K.R., 2003. Artificial neural network based fault diagnostics of rolling element bearings using time-domain features. *Mech. Syst. Signal Process.*, **17**(2):317-328. [doi:10.1006/mssp.2001.1462]
- Selvaganesan, N., Raja, D., Srinivasan, S., Renganathan, S., 2006. Neural Control and Fault Diagnosis for 6/4 Switched Reluctance Motor. IEEE Int. Conf. on Industrial Technology, p.1741-1746. [doi:10.1109/ICIT.2006.372471]
- Selvaganesan, N., Raja, D., Srinivasan, S., 2007. Fuzzy based fault detection and control for 6/4 switched reluctance motor. *Iran. J. Fuzzy Syst.*, **4**(1):37-51.
- Torkaman, H., Afjei, E., 2011. Magnetostatic field analysis and diagnosis of mixed eccentricity fault in switched reluctance motor. *Electromagnetics*, **31**(5):368-383. [doi:10.1080/02726343.2011.579774]
- Torkaman, H., Afjei, E., 2013. Method for eccentricity fault monitoring and diagnosis in switched reluctance machines based on stator voltage signature. *IEEE Trans. Magn.*, **49**(2):912-920. [doi:10.1109/TMAG.2012.2213606]
- Torkaman, H., Afjei, E., Ravaud, R., Lemarquand, G., 2011. Misalignment fault analysis and diagnosis in switched reluctance motor. *Int. J. Appl. Electromagn. Mech.*, **36**(3):253-265. [doi:10.3233/JAE-2011-1364]
- Torkaman, H., Afjei, E., Yadegari, P., 2012. Static, dynamic, and mixed eccentricity faults diagnosis in switched reluctance motors using transient finite element method and experiments. *IEEE Trans. Magn.*, **48**(8):2254-2264. [doi:10.1109/TMAG.2012.2191619]
- Ustun, O., 2009. Investigation of flux and inductance measurement methods of the switched reluctance machines. *SDU Int. J. Technol. Sci.*, **1**(2):21-33 (in Turkish).
- Vas, P., 1993. Parameter Estimation, Condition Monitoring and Diagnosis of Electrical Machines. Oxford University Press, London, UK.
- Vas, P., 1999. Artificial Intelligence Based Electrical Machines and Drives. Oxford University Press, New York, USA.
- Yang, B.S., Han, T., An, J.L., 2004. ART-KOHONEN neural network for fault diagnosis of rotating machinery. *Mech. Syst. Signal Process.*, **18**(3):645-657. [doi:10.1016/S0888-3270(03)00073-6]